Available online at www.sciencedirect.com
ScienceDirect
Trans. Nonferrous Met. Soc. China 31(2021) 3116−3127
Transactions of Nonferrous Metals Society of China
www.tnmsc.cn

Thermodynamic and experimental studies on removal of calcium and sulfate ions from recycling water of complex sulfide flotation operations

Elvis BUSTOS-FLORES, Martha Araceli ELIZONDO-ÁLVAREZ, Alejandro URIBE-SALAS

Department of Metallurgical Engineering, CINVESTAV-IPN, Unidad Saltillo, 25900, Ramos Arizpe, Coahuila, Mexico

Received 8 November 2020; accepted 28 June 2021

Abstract: A chemical method for removing calcium sulfate saturated solutions (0.016 mol/L $CaSO_4$) using barium chloride ($BaCl_2·2H_2O$) and sodium phosphate (Na_3PO_4) was experimentally studied. The main interest is to remove these ions from the solution through the precipitation of two solid species: sulfate (SO_4^{2-}) as barite ($BaSO_4$), and calcium (Ca^{2+}) as hydroxyapatite ($Ca_5(PO_4)_3OH$). Additionally, a solid/liquid separation method (i.e., flotation) was explored, using oleic acid and dodecylamine as collectors. The results show that, the chemical treatment of saturated solutions at 60 °C, pH 11.5 and using 3.9 g/L $BaCl_2·2H_2O$ and 1.6 g/L Na_3PO_4, promotes the precipitation of barium sulfate and calcium-deficient hydroxyapatite ($Ca_{10-x}(HPO_4)_x(PO_4)_{6-x}(OH)_{2-x}$), with residual concentrations of calcium and sulfate below 0.10 and 5 mg/L, respectively. The residual calcium concentration increases to 28 mg/L when using the same amount of reactants, at temperature and pH values below those quoted. The highest flotation recovery of hydroxyapatite with oleic acid at pH 9.5 was about 80%, while that of barite floated with dodecylamine at pH 6.5 was about 90%.
Key words: calcium; sulfate; dodecylamine; oleic acid; barite; hydroxyapatite; flotation separation

1 Introduction

Currently, water has become an increasingly scarce natural resource and it is expected that in the coming decades it will be even more limited. Water consumption by industrial operations of complex sulfides flotation is extremely high [1], which causes the natural sources to be over-exploited, sometimes in an irresponsible manner. To face this scenario, some companies reuse water resources in their processes, which are generally recycled from tailings dams, thickener overflows, and filtration units [2]. However, recycle water commonly contains high concentrations of naturally occurring ions (Na^+, K^+, Mg^{2+}, Ca^{2+}, Cl^-, and CO_3^{2-}) and ions inherent to the process (e.g., Ca^{2+} and SO_4^{2-}, mainly) that alter the chemistry of the system [3,4].

For mineral processing operations with shortage of freshwater, the use of alternative water sources such as recycled water and seawater are realistic options [5−9]. However, the variation of water quality must be carefully considered, as the fluctuation in its composition can drastically change the flotation performance, and this in most cases affects the recovery of the mineral species of interest [10−13].

The presence of calcium in the water of the sulfides flotation operations is due to the use of calcium oxide to raise the pH from around 7 (freshwater pH) to 10 or 11 (in the zinc flotation), as well as to the dissolution of calcium-bearing minerals (i.e., calcite and dolomite) present in the ore. In turn, the presence of sulfate is due to the natural oxidation of the sulfide−sulfur of the minerals [14], due to atmospheric oxygen in contact with the suspension during grinding, conditioning, flotation and thickening, as shown in Reaction 1 [15]. Besides, sulfate also originates from the oxidation of sodium metabisulfite ($Na_2S_2O_5$)

Corresponding author: Martha Araceli ELIZONDO-ÁLVAREZ, E-mail: martha.elizondo.a@gmail.com
DOI: 10.1016/S1003-6326(21)65720-5

that is commonly added as depressant of the sulfide gangue (i.e., pyrite and pyrrhotite) [16]. Table 1 [17−23] presents the sulfate and calcium concentrations of process water of some mining operations around the world, in which it is observed that most of them exceed the saturation concentration for gypsum precipitation (i.e., about 0.016 mol/L). Furthermore, they are all above the limit allowed by WHO or US EPA standard, which is less than 250 mg/L [24].

$$2MeS_2+7O_2+2H_2O\rightarrow 2Me^{2+}+4SO_4^{2-}+4H^+ \quad (1)$$

There are both industrial and laboratory evidences showing that the presence of Ca^{2+} and SO_4^{2-} in sulfide flotation water causes adverse effects on the flotation performance [25−32]. It is worth mentioning that the concentrations of calcium and sulfate ions are critical for mineral depression. BULUT and YENIAL [4] found that galena recovery decreases for concentrations above 1×10^{-3} mol/L (40 and 96 mg/L of Ca^{2+} and SO_4^{2-}, respectively). Similarly, IKUMAPAYI [33] found that galena is gradually depressed in the presence of sulfate concentrations above 100 mg/L. This behavior is probably due to the formation of a non-uniform layer of lead sulfate on the galena surface, which acts as a barrier that hinders the interaction of the collector with the metal sites on the galena surface, inhibiting the chemisorption mechanism [34].

Studies in our laboratories have shown that Ca^{2+} activates sphalerite (ZnS) in the lead circuit, where it must remain in the tails [35]; while SO_4^{2-} depresses galena (PbS) in the Pb−Cu circuit [34]. Furthermore, the simultaneous presence of both ions at concentrations above 0.016 mol/L causes the precipitation of gypsum, which indiscriminately depresses the valuable mineral species (PbS, ZnS, $CuFeS_2$, etc) [36]. It is worth mentioning that the interaction mechanisms between some sulfide minerals and calcium and sulfate ions have been studied by various researchers [34,37−39].

The phenomena described previously resulted in a decrease in the recoveries of the valuable species and the grades of the final concentrates obtained. In order to diminish the adverse effect of calcium and sulfate on flotation, several strategies have been developed to remove them from process water [16,40−42].

The most commonly used method to remove calcium is based on the addition of sodium carbonate as an alkaline agent, with the aim of precipitating it in the form of calcium carbonate, and of dissolving the gypsum that has already precipitated and adhered to mineral surfaces [16]. However, this strategy has the disadvantage that sulfate remains in the solution, which by itself is capable of affecting the collector adsorption on minerals such as galena [24,34]. The feasibility of simultaneously removing calcium and sulfate has been studied through the use of compounds based on calcium aluminate, with the aim of precipitating calcium sulfate as ettringite, a hydrated calcium sulfoaluminate, achieving residual concentrations of calcium and sulfate below 200 mg/L [40]. Besides, electrochemical methods such as electrocoagulation for calcium and sulfate removal have been studied and developed in recent years [15,19,43,44]. However, these are still under development and one of their main disadvantages, in addition to anodic passivation, is the high energy consumption.

Table 1 Sulfate and calcium concentrations of process water of some mining operations around world [17−23]

Localization	Type of mine	Concentration/ ($mg\cdot L^{-1}$)		Strategy of removal	Ref.
		Sulfate	Calcium		
Harmony Mine, South Africa	Gold	4800	1040	CSIR ABC (alkali−barium−calcium) desalination process	[17]
Abandoned Mine Guanajuato, Mexico	Silver	3567	−	Electrocoagulation	[18]
Copper Mine, China	Copper	3000	−	Sulfate-reducing bacteria (SRB) process	[19]
Carnoule's Mine, France (inactive)	Lead−zinc	2000−7500	−	Sulfate-reducing bacteria (SRB) process	[20]
Chessy Mines, France	Copper	5000	−	Sulfate-reducing bacteria (SRB) process	[21]
Nickel Rim Mine Site, Canada	Nickel	2400−4600	2300	A permeable reactive wall	[22]
Avoca Mines, Ireland	Copper	10579	−	−	[23]

Based on the previous studies described above, it is important and relevant to treat recycling water, under the diverse circumstances that arise in the polymetallic sulfide flotation circuits. In the present investigation, a chemical method to remove calcium and sulfate ions is experimentally studied, through the precipitation of barium sulfate and calcium phosphate from a synthetic solution with concentrations and pH similar to those found in process water, namely, saturated with calcium sulfate and alkaline pH. Likewise, barium sulfate ($BaSO_4$) and calcium phosphate (hydroxyapatite, $CaHPO_4$, or another similar compound) were obtained as by-products. Figure 1 illustrates the process applied in complex sulfide flotation operations that recirculate process water from thickener/tailings dam.

2 Experimental

2.1 Materials

The synthetic solution used in this work was a saturated calcium sulfate solution (0.016 mol/L) in equilibrium with calcium sulfate dihydrate ($CaSO_4·2H_2O$). The reactants that were used to treat the saturated solution were barium chloride ($BaCl_2·2H_2O$) and sodium phosphate (Na_3PO_4). As pH regulators, solutions of hydrochloric acid (HCl) and sodium hydroxide (NaOH) were used. Oleic acid and dodecylamine (DDA) were used in the microflotation measurements as hydroxyapatite and barite collectors, respectively. The chemical structures of both collectors are illustrated in Fig. 2. It is worth mentioning that all the reagents and

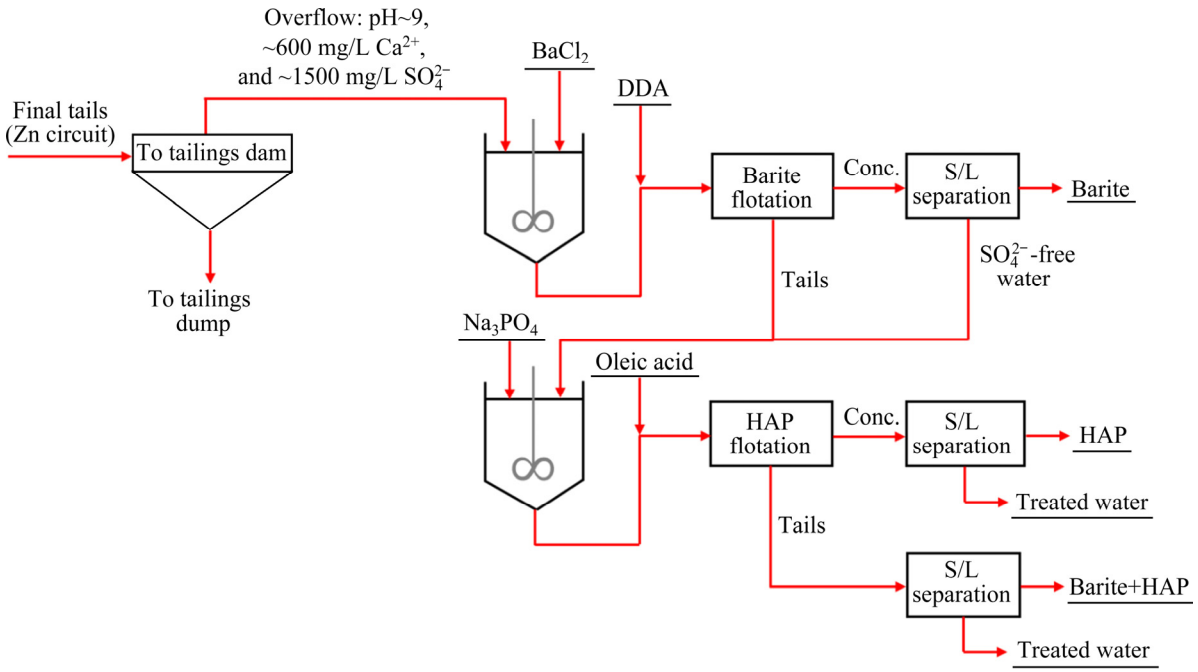

Fig. 1 Process to remove calcium and sulfate in complex-sulfide flotation operations that recirculate process water from thickener/tailings dam

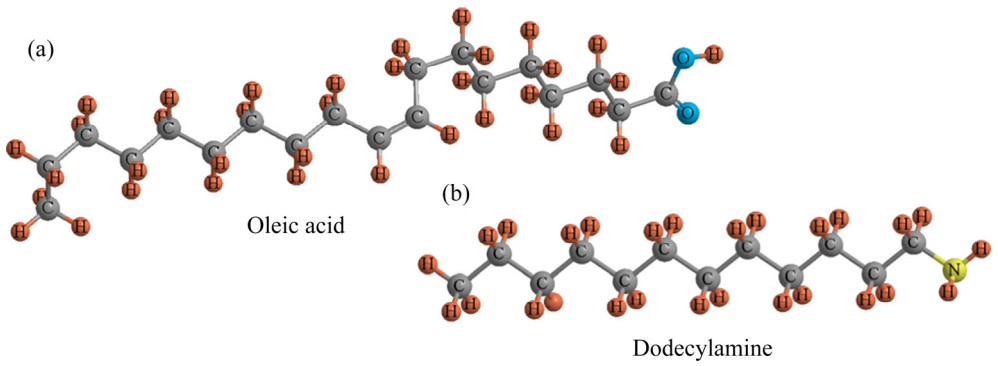

Fig. 2 Chemical structures of collectors: (a) Oleic acid; (b) Dodecylamine

collectors used were analytical grade and were supplied by Sigma Aldrich.

2.2 Thermodynamic simulation of aqueous systems of interest

The conducted thermodynamic modeling has two aspects: the first focuses on determining the solubility of $CaSO_4·2H_2O$ (i.e., the concentration of calcium and sulfate species at the saturation point), and the second is aimed at establishing the amount of the necessary reactant for precipitating barite ($BaSO_4$), of very low solubility, due to the reaction of added $BaCl_2·2H_2O$ and the sulfate species ($CaSO_{4(aq)}$, SO_4^{2-} and HSO_4^-) of a saturated solution (0.016 mol/L $CaSO_4$); the second focuses on the precipitation of some species of calcium phosphate (HAP: $Ca_5(PO_4)_3OH$), also of low solubility, due to the reaction between the added sodium phosphate and the calcium species ($CaSO_{4(aq)}$, Ca^{2+} and $CaOH^+$) of a saturated solution. Thermodynamic modeling was carried out at pH 11.5.

The thermodynamic modeling was performed at 25 °C considering the following species: in the case of gypsum solubility, $H_2O_{(l)}$, H^+, OH^-, $CaSO_4·2H_2O_{(s)}$, $CaSO_{4(aq)}$, Ca^{2+}, $CaOH^+$, SO_4^{2-} and HSO_4^-; in the case of barite precipitation, $BaSO_{4(s)}$, Ba^{2+}, $BaOH^+$, $BaCl^+$, Cl^-, $CaCl^+$, $CaCl_{2(aq)}$, $BaCl_2·2H_2O_{(s)}$ (added reactant), $Ca(OH)_{2(s)}$ and $Ba(OH)_{2(s)}$, in addition to the species of the gypsum−water system; in the case of "hydroxyapatite" precipitation, $Ca_5(PO_4)_3OH_{(s)}$, $Ca_3(PO_4)_{2(s)}$ $CaHPO_{4(s)}$, $3Ca_3(PO_4)_2·Ca(OH)_{2(s)}$, $Na_3PO_{4(s)}$ (added reactant), $Ca_3(PO_4)_{2(aq)}$, $Ca_5(PO_4)_3OH_{(aq)}$, PO_4^{3-}, HPO_4^{2-}, $H_2PO_4^-$, $H_3PO_{4(aq)}$, Na^+ and $NaSO_4^-$, in addition to the species of the gypsum−water system. A relatively small volume atmosphere (79% N_2, 21% O_2, 0.03% CO_2, volume fraction) was considered to facilitate the convergence of the thermodynamic calculations of the system. The evolution of the concentration of chemical species in equilibrium, in aqueous and solid states, was plotted as a function of the amount of added reactant. The modeling was performed with the HSC Chemistry 6.1 thermodynamic software.

It is important to achieve a more accurate prediction of a system that involves a non-ideal solution, the activity coefficients of the aqueous species present in the solution were estimated using Davies' equation (Eq. (2)), as a function of the ionic strength of the solution (Eq. (2)):

$$-\lg \gamma = Az^2\left(\frac{\sqrt{I}}{1+\sqrt{I}} - BI\right) \tag{2}$$

where γ is the activity coefficient, A and B are temperature-dependent constants (at 25 °C, A and B take values of 0.509 and 0.328, respectively), z is the valence of the aqueous species, and I represents the ionic strength of the solution, which is estimated with Eq. (3):

$$I = \frac{1}{2}\sum c_i z_i^2 \tag{3}$$

where c_i and z_i are the concentration (mol/L) and the valence of species i, respectively.

The activity coefficients calculated for the $CaSO_4·2H_2O$ system are as follows: $\gamma^{1\pm}$=0.8239, $\gamma^{2\pm}$=0.4609.

These coefficients are used in both systems of calcium and sulfate precipitation since both consider the treatment of a saturated calcium sulfate solution for which these activity coefficients are applied.

2.3 Calcium and sulfate removal measurements

Calcium and sulfate removal measurements were carried out in a water-jacketed beaker containing 1 L of the saturated solution of $CaSO_4$ (0.016 mol/L), at 25 °C and pH 7.5 or 11.5. It should be noted that this solution is a simplified but approximate representation of the process water of complex sulfide concentrators, which is generally saturated with gypsum and shows a slightly alkaline pH (between 8 and 11), so its content of dissolved heavy metals is very low (i.e., these have precipitated as solid metal hydroxides).

The removal of sulfate and calcium ions in the form of $BaSO_4$ or $Ca_5(PO_4)_3OH$ was carried out in two stages: in the first stage, the necessary amount of the reactant $BaCl_2·2H_2O$ or Na_3PO_4 was added (according to the amount resulting from the thermodynamic modeling) to the saturated solution; after 1 h of vigorous stirring, the solids obtained were filtered and separated. In the second stage, the second reactant (Na_3PO_4 or $BaCl_2·2H_2O$) was added to the filtered solution and after 1 h of agitation, the suspension was filtered and the solids were dried at room temperature.

2.4 Characterization of reaction products

The solid products of the chemical reactions were filtered, dried at room temperature, and analyzed by X-ray diffraction (XRD) using a D8 Advance Bruker diffractometer. Likewise, the precipitates were analyzed by plasma emission spectroscopy (ICP-OES) using a PerkinElmer spectrophotometer (Optima 8300) to determine their calcium and phosphorus concentrations.

2.5 Analysis methods for determination of calcium and sulfate ions

The filtered solutions were chemically analyzed to determine calcium and sulfate residual concentrations. The quantification of sulfate in solution was carried out using the turbidimetric method, which corresponds to the ASTM D516—02 standard, for which a LaMotte 2020i turbidimeter was used. The residual calcium concentration was determined by ICP, using a PerkinElmer spectrophotometer (Optima 8300).

2.6 Zeta potential measurements

The zeta potential measurements were carried out using a Pen Kem model 501 zetameter, which allows direct reading of the zeta potential of colloidal particles, estimated with their electrophoretic mobility and the Smoluchowski equation [45]. The investigated pH range was from 4 to 10; in all cases, particles below 20 μm were used. To determine the zeta potential of hydroxyapatite and barite in water, 0.15 g of mineral was conditioned for 10 min in deionized water at different pH (from 2 to 10). Next, a sample of the suspension was taken, and the zeta potential was measured. The pH was controlled by means of 0.1 mol/L NaOH and HCl solutions. The experiments were triplicate and the average recovery was reported together with the error bars of the 95% confidence interval of a Student's t-distribution [46].

2.7 Microflotation experiments

Microflotation tests were conducted in an 80 mL Partridge-Smith cell using 1 g of sample (hydroxyapatite or barite) with the size fraction of 75−106 μm, which was conditioned for 5 min in 100 mL of the collector solution (oleic acid or dodecylamine), at the concentration and pH of interest. Next, the solid sample and 80 mL of the solution were transferred to the cell and the solids were floated for 4 min with 23 mL/min of high purity nitrogen. The remaining solution (20 mL) was progressively added to the cell as make-up water. At the end of the test, the floated and sunk solids were filtered, dried, and weighed, to calculate the recovery. The experiments were triplicate, and the average recovery was reported together with the error bars of the 95% confidence interval of a Student's t-distribution.

3 Results and discussion

3.1 Gypsum ($CaSO_4·2H_2O$) solubility

Figure 3 shows the species distribution diagram of calcium sulfate species in aqueous solution to which accumulative amounts of gypsum ($CaSO_4·2H_2O$) were added. It is clearly observed in the figure that gypsum ceases to dissolve at a $CaSO_4·2H_2O$ concentration of approximately 0.016 mol/L. It should be noted that this modeling corroborates the experimentally measured concentration of the saturated solution used in this study.

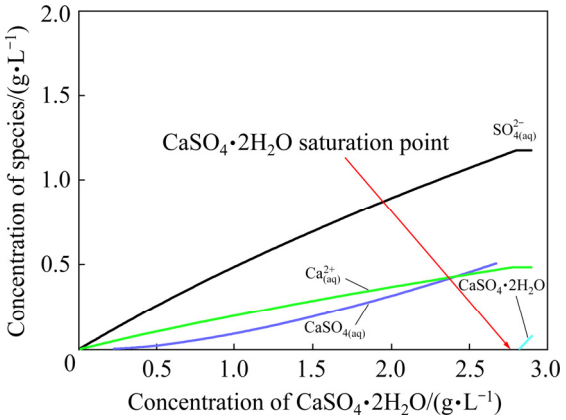

Fig. 3 Species distribution diagram of $CaSO_4$–H_2O system at 25 °C open to atmosphere (79.02% N_2, 20.94% O_2, 0.03% CO_2)

3.2 Necessary amount of reactants for $BaSO_4$ and HAP precipitation

Figure 4 shows the species distribution diagram of the systems analyzed considering 1 L of saturated solution of $CaSO_4·2H_2O$ (0.016 mol/L), when barium chloride (Fig. 4(a)) and sodium phosphate (Fig. 4(b)) are added, for which the following reactions are suggested to occur:

$$CaSO_{4(aq)}+BaCl_{2(s)}\rightarrow BaSO_{4(s)}+CaCl_{2(aq)} \quad (4)$$

$$CaSO_{4(aq)}+\frac{2}{3}Na_3PO_{4(s)}+\frac{2}{15}H_2O_{(aq)}+\frac{1}{15}OH^-_{(aq)}\rightarrow \frac{1}{5}Ca_5(PO_4)_3OH_{(s)}+Na_2SO_{4(aq)}+\frac{1}{15}H_2PO^-_{4(aq)} \quad (5)$$

In Fig. 4(a) it is clearly observed that the precipitation of the SO_4^{2-} as $BaSO_4$ is achieved by adding approximately 3.9 g of reactant $BaCl_2·2H_2O$. In turn, the precipitation of hydroxyapatite ($Ca_5(PO_4)_3OH$) is achieved with addition of approximately 1.6 g of Na_3PO_4 (see Fig. 4(b)).

Once the necessary amounts of the reactants for the complete removal of sulfate and calcium were determined, the way of adding them (i.e., in a single dose or cumulative fractions of the does), the effects of pH and temperature on the residual concentrations of calcium and sulfate, as well as on the crystallinity of the precipitates were evaluated. The results obtained are presented and discussed below.

3.3 Removal of calcium and sulfate from saturated solution (0.016 mol/L $CaSO_4$)

Table 2 presents the initial concentrations of the calcium and sulfate ions in the saturated solution, as well as the residual concentration after chemical treatment under different conditions. The table shows that regardless of the order and mode of addition of the reactants, as well as of the temperature and pH used, the residual sulfate concentration is below 5 mg/L, which confirms the effective removal of the SO_4^{2-} in all tests.

It is worth noting that the lowest residual calcium concentration (<0.10 mg/L) is obtained in Test 2, which consists of treating the saturated solution at pH 11.5 and 60 °C, by adding Na_3PO_4 in a single dose, while $BaCl_2$ is cumulatively added in five fractions of the dose. Note that when using

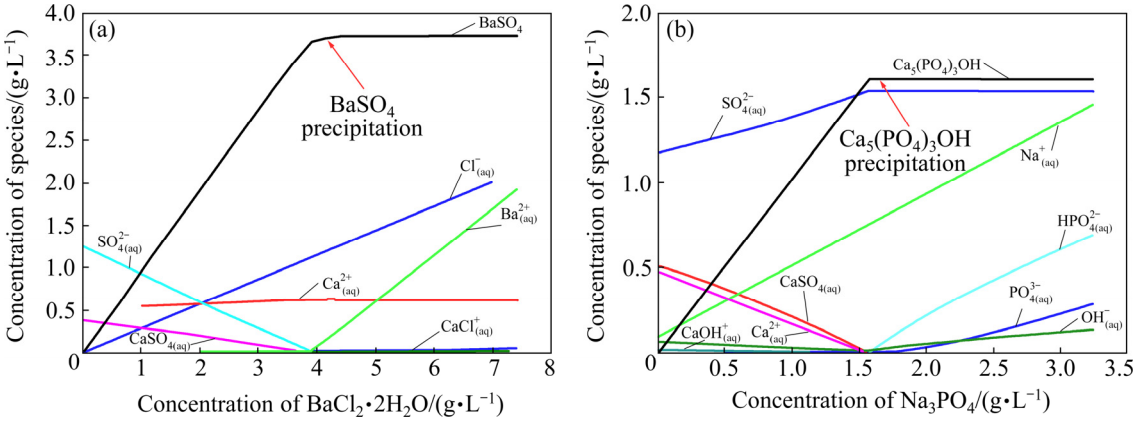

Fig. 4 Species distribution diagrams of systems of $CaSO_4$–$BaCl_2·2H_2O$ and (b) $CaSO_4$–Na_3PO_4 (b) (Systems were analyzed based on 1 L of saturated solution of $CaSO_4·2H_2O$ (0.016 mol/L), 25 °C and in atmosphere (79.02% N_2, 20.94% O_2, 0.03% CO_2, volume fraction)

Table 2 Initial concentrations of sulfate and calcium ions in saturated solution (0.016 mol/L $CaSO_4·2H_2O$) and residual concentrations after chemical treatment under different conditions

Test No.	Initial concentration/(mg·L^{-1})		Experimental condition					Residual concentration/(mg·L^{-1})	
	Ca^{2+}	SO_4^{2-}	T/°C	pH	Amount of $BaCl_2·H_2O$/g	Amount of Na_3PO_4/g	Order of reactants addition	Ca^{2+}	SO_4^{2-}
1	641	1536	35	11.6	3.9	1.6	(1) Na_3PO_4 *; (2) $BaCl_2$ *	3.8	<5
2	641	1536	60	11.6	3.9	1.6	(1) Na_3PO_4 (single dose); (2) $BaCl_2$ *	<0.10	<5
3	641	1536	25	7.5	3.9	1.6	(1) Na_3PO_4 (single dose); (2) $BaCl_2$ *	28	<5
4	641	1536	25	11.6	3.9	1.6	Simultaneous addition (single dose)	23	<5
5	641	1536	25	11.6	3.9	1.6	(1) Na_3PO_4 **; (2) $BaCl_2$ *	5.5	<5

*Reactant added in 5 cumulative additions; **Reactant added in 10 cumulative additions

the same reactants and pH, and the temperature is increased from 25 to 35 °C, the remaining calcium concentration decreases from 5.5 to 3.8 mg/L. Furthermore, the residual calcium concentration is further increased to 28 mg/L when using the same reactants, but the lower values of temperature and pH (i.e., 25 °C and pH 7.5).

3.4 XRD patterns of precipitates

Based on the qualitative behavior of the test shown and discussed previously, the precipitates from Test 2 were selected to be characterized by X-ray diffraction (XRD). The diffractograms are shown in Fig. 5.

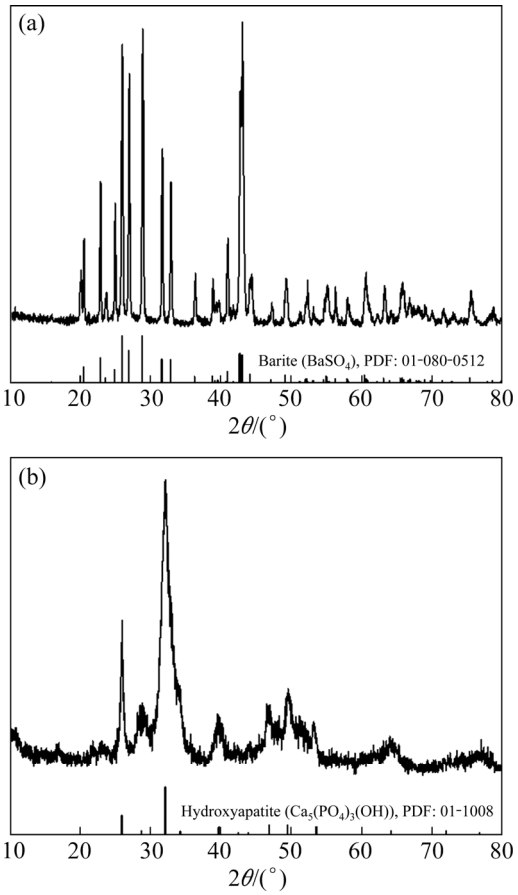

Fig. 5 XRD patterns of precipitates obtained from Test 2: (a) Barite; (b) Hydroxyapatite

The characteristic peaks observed correspond to barite and hydroxyapatite, which are identified with the diffraction patterns 01-080-0512 and 01-1008, respectively. It should be noted that no other phase was identified, indicating that the precipitates obtained are practically pure. It is important to note that unlike barite, very broad peaks are observed in the XRD patterns of hydroxyapatite, which suggests that the obtained HAP is fairly amorphous.

It should be noted that these results give the guideline to explore different experimental conditions to obtain a more crystalline hydroxyapatite. This may be probably achieved by considering the growth of the particles by controlling the additions of reagents, as well as a subsequent heat treatment at moderate temperatures.

3.5 Calcium and phosphorus determination by ICP-OES

Table 3 presents the results of elemental analysis by ICP-OES of the hydroxyapatite precipitate from Test 2, in which a Ca/P molar ratio of 1.50:1 was obtained, which corresponds to a mass ratio of around 2:1. In this regard, a series of molar relationships are reported in Ref. [47], which are related to the occurrence of different calcium phosphate species. Based on this classification, it is inferred that the analyzed precipitate corresponds to a calcium-deficient hydroxyapatite, $Ca_{10-x}(HPO_4)_x(PO_4)_{6-x}(OH)_{2-x}$ ($0<x<1$), stable at pH between 6.5 and 9.5 [47]. The latter may explain the behavior of the solids when measuring their zeta potentials at pH below 5.5, since the particles were neither clearly appreciated, nor their movement could be accurately measured, as will be discussed later.

Table 3 Elemental analysis results of hydroxyapatite precipitate obtained in Test 2 by ICP-OES

Element	Content/wt.%	Ca/P molar ratio
Ca	20.90	1.50:1
P	10.71	

3.6 Zeta potentials of barite and hydroxyapatite

Zeta potential measurements were carried out in order to determine surface charges of the barite and hydroxyapatite particles in the pH range of interest, before conditioning with the collectors. Fig. 6 presents the results obtained.

In the case of barite, it is observed that the particles present their isoelectric point at pH around 2, similar to that reported by REN et al [48]. This value is of relevance since under this condition it is expected that the flocculation of fine particles may occur. It is also observed that the charge of barite particles becomes more negative as the suspension pH increases. Furthermore, in the pH range between

4 and 6, a region of fairly constant potential is observed, which is probably due to the predominance of the $BaHCO_3^+$ species on the barite surface, according to the thermodynamic modeling of the system (see Fig. 7). Finally, at pH values above 7, the zeta potential becomes more negative, probably due to the action of the incongruent dissolution mechanism, which favors the dissolution of Ba^{2+} over SO_4^{2-}, thus leaving a surface enriched with sulfate, which provides his negative character to the particle (see Fig. 7(b)).

In the case of hydroxyapatite, measurements below pH 5 were not possible because the solid particles and their movement could not be clearly appreciated. This behavior is attributed to the nature of the solid, identified as Ca-deficient hydroxyapatite ($Ca_{10-x}(HPO_4)_x(PO_4)_{6-x}(OH)_{2-x}$), stable at pH between 6.5 and 9.5 [47]. In Fig. 6(b), it is observed that the surface of HAP gradually becomes negatively charged as the pH increases from 5.5 to 10. The mechanism of surface charge development is also incongruent dissolution, with calcium dissolving in excess to phosphate mainly due to the formation of calcium hydroxo complex ($CaOH^+$).

Based on the information obtained with the zeta potential measurements, we explore flotation as the solid/liquid separation method. It should be noted that there are other separation methods such as those based on flocculation, in which resultant precipitates are removed by either sedimentation or filtration [49]. However, it is important to note that this method may be easy only for barite, whose isoelectric point occurs at pH around 2 (see Fig. 6(a)). In the case of the calcium-deficient hydroxyapatite ($Ca_{10-x}(HPO_4)_x(PO_4)_{6-x}(OH)_{2-x}$), the flocculation of particles could be difficult since they present a surface negative charge.

3.7 Microflotation results of barite and hydroxyapatite

The cationic collector dodecylamine ($R—NH_2$) and the anionic collector oleic acid (R—COOH) were selected to conduct the microflotation tests.

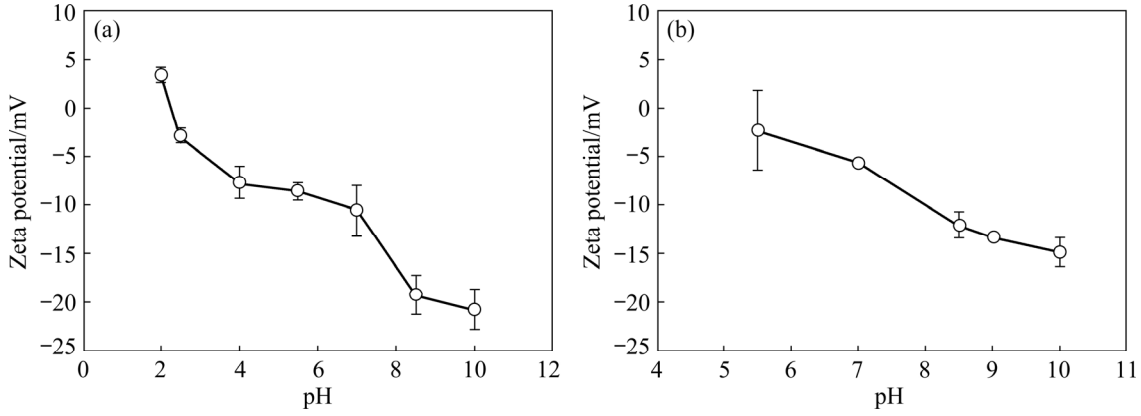

Fig. 6 Zeta potentials of barite (a) and hydroxyapatite (b) as function of pH (The error bars correspond to the 95% confidence intervals)

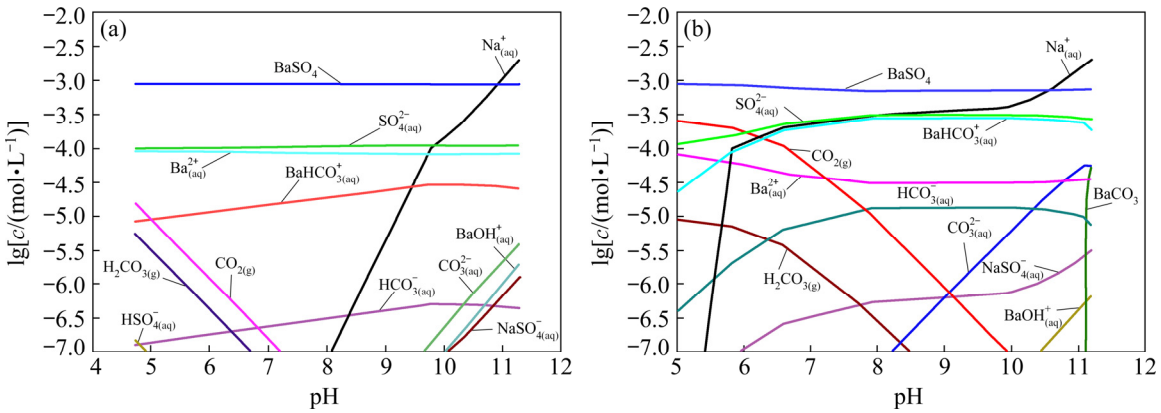

Fig. 7 Species distribution diagram of $BaSO_4$–H_2O–O_2–CO_2 system (10 g/L $BaSO_4$) at 25 °C in atmosphere (79.02% N_2, 20.94% O_2 and 0.03% CO_2): (a) Initial states; (b) Equilibrium

Hydroxyapatite microflotation was performed using two concentrations of oleic acid (5×10^{-4} and 5×10^{-5} mol/L) and two size fractions (75−106 μm and <75 μm). The results obtained are presented in Fig. 8. It is observed that regardless of the particle size and the collector concentration used, the recovery is favored at pH 9.5. This behavior has to do with the dissociation of the collector, since at pH values below 8 the neutral species R—COOH predominates, while at higher pH values the ion $R—COO^-$ and its dimmer $(R—COO^-)_2^{2-}$ predominate [50,51]. Apparently, these ions ($R—COO^-$ and $(R—COO^-)_2^{2-}$) are the ones that chemically interact with the positive sites of hydroxyapatite, Ca^{2+} and $CaOH^+$, providing HAP the hydrophobic properties necessary to be recovered by the gas bubbles. The highest hydroxyapatite recovery, around 80%, was obtained at pH 9.5 using the size fraction of 75−106 μm and 5×10^{-4} mol/L of collector.

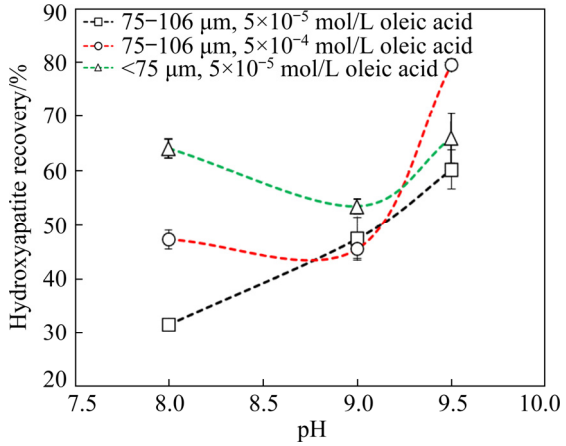

Fig. 8 Effect of pH and oleic acid concentration on hydroxyapatite recovery (The mineral was conditioned for 4 min in 200 mL of the oleic acid solution and subsequently floated for 4 min at room temperature)

Figure 9 shows the recovery of barite as a function of pH. The figure shows that the recovery increases as the pH decreases from 9.5 to 6.5, which is attributed to the fact that the RNH_3^+ cation favorably interacts with the negatively charged barite particle. At the collector concentration tested, the cation RNH_3^+ predominates at pH below 10 [52]. As observed in the figure, the highest recovery of barite, around 88%, was obtained at pH 6.5, where barium sulfate ($BaSO_4$) is the most stable species (see Fig. 7). Above this pH value, the $BaHCO_3^+$ species forming in the double-layer that surrounds the barite particle (see Fig. 7), may interfere with the adsorption of the cationic collector, thus reducing the particle hydrophobicity.

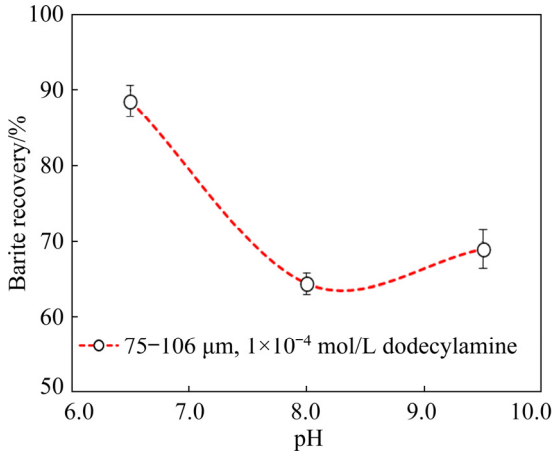

Fig. 9 Effect of pH on recovery of barite (The mineral was conditioned for 4 min in 200 mL of 1×10^{-4} mol/L dodecylamine, after being floated for 4 min)

4 Conclusions

(1) Based on the thermodynamic simulations, the best conditions for the removal of Ca^{2+} and SO_4^{2-} ions were determined and experimentally corroborated. The chemical treatment of $CaSO_4$ saturated solutions at 60 °C, pH 11.5 and treated with 3.9 g/L of $BaCl_2\cdot2H_2O$ and 1.6 g/L of Na_3PO_4, promotes the precipitation of barium sulfate ($BaSO_4$) and calcium-deficient hydroxyapatite ($Ca_{10-x}(HPO_4)_x(PO_4)_{6-x}(OH)_{2-x}$), with the residual concentrations below 0.10 and 5 mg/L of calcium and sulfate, respectively.

(2) The calcium-deficient hydroxyapatite ($Ca_{10-x}(HPO_4)_x(PO_4)_{6-x}(OH)_{2-x}$) was obtained, although the possible formation of another calcium phosphate of relatively amorphous nature was not discarded.

(3) The highest flotation recovery of hydroxyapatite with oleic acid at pH 9.5 was about 80%, while that of barite floated with dodecylamine at pH 6.5 was about 88%. Oleic acid species $C_{17}H_{33}COO^-$ and $(C_{17}H_{33}COO)_2^{2-}$ chemically interact with the positive sites of hydroxyapatite, Ca^{2+} and $CaOH^+$; apparently, both are responsible for the maximum recovery attained under such conditions. In turn, the recovery of barite was relatively easy, most probably due to the favorable interaction between the RNH_3^+ cation and the negatively charged barite surface.

(4) The mineral processing industry is expected to adopt chemical treatment more decidedly due to its simplicity and inexpensive nature.

Acknowledgments

The authors are grateful for the financial supports from the personnel of Cinvestav-IPN Unidad Saltillo as well as the scholarships awarded by CONACYT (México).

References

[1] LI Y, XIE S, ZHAO Y, XIA L, LI H, SONG S. The life cycle of water used in flotation: A review [J]. Mining, Metallurgy & Exploration, 2019, 36: 385−397.

[2] JOHNSON N W. Issues in maximation of recycling of water in a mineral processing plant [C]//Proc Water in Mining, Brisbane, Australia. Australasian Institute of Mining and Metallurgy, 2003: 239−245.

[3] BIÇAK Ö, EKMEKÇI Z, CAN M, ÖZTÜRK Y. The effect of water chemistry on froth stability and surface chemistry of the flotation of a Cu−Zn sulfide ore [J]. International Journal of Mineral Processing, 2012, 102−103: 32−37.

[4] BULUT G, YENIAL Ü. Effects of major ions in recycled water on sulfide minerals flotation [J]. Minerals & Metallurgical Processing, 2016, 33: 137−143.

[5] JELDRES R I, FORBES L, CISTERNAS L A. Effect of seawater on sulfide ore flotation: A review [J]. Mineral Processing and Extractive Metallurgy Review, 2016, 37: 369−384.

[6] JELDRES R I, ARANCIBIA-BRAVO M P, REYES A, AGUIRRE C E, CORTES L, CISTERNAS L A. The impact of seawater with calcium and magnesium removal for the flotation of copper−molybdenum sulphide ores [J]. Minerals Engineering, 2017, 109: 10−13.

[7] JELDRES R I, CALISAYA D, CISTERNAS L A. An improved flotation test method and pyrite depression by an organic reagent during flotation in seawater [J]. Journal of the Southern African Institute of Mining and Metallurgy, 2017, 117: 499−504.

[8] MORENO P A, ARAL H, CUEVAS J, MONARDES A, ADARO M, NORGATE T, BRUCKARD W. The use of seawater as process water at Las Luces copper–molybdenum beneficiation plant in Taltal (Chile) [J]. Minerals Engineering, 2011, 24: 852−858.

[9] REBOLLEDO E, LASKOWSKI J S, GUTIERREZ L, CASTRO S. Use of dispersants in flotation of molybdenite in seawater [J]. Minerals Engineering, 2017, 100: 71−74.

[10] SHENGO L M, GAYDARDZHIEV S, KALENGA N M. Malachite and heterogenite behavior during the locked-cycle recycling of process water in flotation of copper−cobalt oxide ores [J]. International Journal of Mineral Processing, 2016, 157: 152−162.

[11] RAO S R, FINCH J A. A review of water re-use in flotation [J]. Minerals Engineering, 1989, 2: 65−85.

[12] LEVAY G, SMART R S C, SKINNER W M. The impact of water quality on flotation performance [J]. Journal of the Southern African Institute of Mining and Metallurgy, 2001, 101: 69−75.

[13] SHENGO L M, GAYDARDZHIEV S, KALENGA N M. Effects of process water recycling during flotation of copper and cobalt oxidised ores from Luiswishi deposit in the Democratic Republic of Congo [J]. Desalination and Water Treatment, 2016, 57: 15326−15342.

[14] SÁNCHEZ-ANDREA I, SANZ J L, BIJMANS M F M, STAMS A J M. Sulfate reduction at low pH to remediate acid mine drainage [J]. Journal of Hazardous Materials, 2014, 269: 98−109.

[15] MAMELKINA M A, COTILLAS S, LACASA E, SÁEZ C, TUUNILA R, SILLANPÄÄ M, HÄKKINEN A, RODRIGO M A. Removal of sulfate from mining waters by electrocoagulation [J]. Separation and Purification Technology, 2017, 182: 87−93.

[16] GRANO S R, WONG P L M, SKINNER W, JOHNSON N W, RALSTON J. Detection and control of calcium sulfate precipitation in the lead circuit of the Hilton concentrator of Mount Isa Mines Limited [C]//Proc XIX IMPC. Colorado, USA: Society for Mining, Metallurgy & Exploration, 1995: 171−179.

[17] MOTAUNG S, MAREE J, de BEER M, BOLOGO L, THERON D, BALOYI J. Recovery of drinking water and by-products from gold mine effluents [J]. International Journal of Water Resources Development, 2008, 24: 433−450.

[18] ANGEL P, CARREÑO AGUILERA G, NAVA J, MARTÍNEZ M T, ORTIZ J. Removal of arsenic and sulfates from an abandoned mine drainage by electrocoagulation: Influence of hydrodynamic and current density [J]. International Journal of Electrochemical Science, 2014, 9: 710−719.

[19] HE B, YANG K, QUAN H G, YANG H, TIAO S J, YING F. Treatment of acid mine drainage by sulfate reducing bacteria with iron in bench scale runs [J]. Bioresource Technology, 2013, 128: 818−822.

[20] GILOTEAUX L, DURAN R, CASIOT C, BRUNEEL O, ELBAZ-POULICHET F, GOÑI-URRIZA M. Three-year survey of sulfate-reducing bacteria community structure in Carnoulès acid mine drainage (France), highly contaminated by arsenic [J]. FEMS Microbiology Ecology, 2013, 83: 724−737.

[21] FOUCHER S, BATTAGLIA-BRUNET F, IGNATIADIS I, MORIN D. Treatment by sulfate reducing bacteria of Chessy acid mine drainage and metal recovery [J]. Chemical Engineering Science, 2001, 56: 1639−1645.

[22] BENNER S G, BLOWES D W, PTACEK C J. A full-scale porous reactive wall for prevention of acid mine drainage [J]. Groundwater Monitoring & Remediation, 1997, 17: 99−107.

[23] GRAY N F. Field assessment of acid mine drainage contamination in surface and ground water [J]. Environmental Geology, 1996, 27: 358−361.

[24] FERNANDO W A M, ILANKOON I M S K, SYED T H, YELLISHETTY M. Challenges and opportunities in the removal of sulphate ions in contaminated mine water: A review [J]. Minerals Engineering, 2018, 117: 74−90.

[25] IKUMAPAYI F, MAKITALO M, JOHANSSON B, RAO K. Recycling process water in sulfide flotation. Part A: Effect of calcium and sulfate on sphalerite recovery [J]. Minerals and Metallurgical Processing, 2012, 29: 183−191.

[26] IKUMAPAYI F, RAO K H. Recycling process water in complex sulfide ore flotation: Effect of calcium and sulfate on sulfide minerals recovery [J]. Mineral Processing and Extractive Metallurgy Review, 2015, 36: 45−64.

[27] IKUMAPAYI F, MAKITALO M, JOHANSSON B, RAO K H. Recycling of process water in sulphide flotation: Effect of calcium and sulphate ions on flotation of galena [J]. Minerals Engineering, 212, 39: 77−88.

[28] LASCELLES D, FINCH J A, SUI C. Depressant action of Ca and Mg on flotation of Cu activated sphalerite [J]. Canadian Metallurgical Quarterly, 2003, 42: 133−140.

[29] LIU Q, ZHANG Y. Effect of calcium ions and citric acid on the flotation separation of chalcopyrite from galena using dextrin [J]. Minerals Engineering, 2000, 13: 1405−1416.

[30] PIANTADOSI C, SMART R S C. Statistical comparison of hydrophobic and hydrophilic species on galena and pyrite particles in flotation concentrates and tails from TOF-SIMS evidence [J]. International Journal of Mineral Processing, 2002, 64: 43−54.

[31] SHAHVERDI M R, KHODADADI DARBAN A, ABDOLLAHY M, YAMINI Y. Investigation of effect of sulfate ion on xanthate consumption in galena flotation based on thermodynamic diagrams [J]. Journal of Mining and Environment, 2018, 9: 1035−1048.

[32] GRANO S R, LAUDER D W, JOHNSON N W, RALSTON J. An investigation of galena recovery problems in the Hilton concentrator of Mount Isa Mines Limited, Australia [J]. Minerals Engineering, 1997, 10: 1139−1163.

[33] IKUMAPAYI F. Flotation chemistry of complex sulphide ores: Recycling of process water and flotation selectivity [D]. Luleå: Luleå University of Technology, 2010.

[34] ELIZONDO-ÁLVAREZ M A, FLORES-ÁLVAREZ J M, DÁVILA-PULIDO G I, URIBE-SALAS A. Interaction mechanism between galena and calcium and sulfate ions [J]. Minerals Engineering, 2017, 111: 116−123.

[35] DÁVILA-PULIDO G I, URIBE-SALAS A, ÁLVAREZ-SILVA M, LÓPEZ-SAUCEDO F. The role of calcium in xanthate adsorption onto sphalerite [J]. Minerals Engineering, 2015, 71: 113−119.

[36] DÁVILA-PULIDO G I, URIBE-SALAS A. Effect of calcium, sulphate and gypsum on copper-activated and non-activated sphalerite surface properties [J]. Minerals Engineering, 2014, 55: 147−153.

[37] SUI C, RASHCHI F, XU Z, KIM J, NESSET J E, FINCH J A. Interactions in the sphalerite $Ca-SO_4-CO_3$ systems [J]. Colloids and Surfaces A: Physicochemical and Engineering Aspects, 1998, 137: 69−77.

[38] FLORES-ÁLVAREZ J M, ELIZONDO-ÁLVAREZ M A, DÁVILA-PULIDO G I, GUERRERO-FLORES A D, URIBE-SALAS A. Electrochemical behavior of galena in the presence of calcium and sulfate ions [J]. Minerals Engineering, 2017, 111: 158−166.

[39] OCTOBER L L, CORIN K C, MANONO M S, SCHREITHOFER N, WIESE J G. A fundamental study considering specific ion effects on the attachment of sulfide minerals to air bubbles [J]. Minerals Engineering, 2020, 151: 106313.

[40] GUERRERO-FLORES A D, URIBE-SALAS A, DÁVILA-PULIDO G I, FLORES-ÁLVAREZ J M. Simultaneous removal of calcium and sulfate ions from flotation water of complex sulfides [J]. Minerals Engineering, 2018, 123: 28−34.

[41] MAZUELOS A, IGLESIAS-GONZÁLEZ N, MONTES-ROSÚA C, LORENZO-TALLAFIGO J, ROMERO R, CARRANZA F. A new thiosalt depuration bioprocess for water-recycling in metallic sulphide mineral processing [J]. Minerals Engineering, 2019, 143: 106031.

[42] CHANG L P, CAO Y J, FAN G X, LI C, PENG W J. A review of the applications of ion floatation: Wastewater treatment, mineral beneficiation and hydrometallurgy [J]. RSC Advances, 2019, 9: 20226−20239.

[43] MAMELKINA M A, TUUNILA R, SILLÄNPÄÄ M, HÄKKINEN A. Systematic study on sulfate removal from mining waters by electrocoagulation [J]. Separation and Purification Technology, 2019, 216: 43−50.

[44] MOLLAH M Y A, MORKOVSKY P, GOMES J A G, KESMEZ M, PARGA J, COCKE D L. Fundamentals, present and future perspectives of electrocoagulation [J]. Journal of Hazardous Materials, 2004, 114: 199−210.

[45] DELGADO Á V. Interfacial electrokinetics and electrophoresis [M]. New York: John Wiley & Sons, Inc, 2002.

[46] MONTGOMERY D C. Design and Analysis of Experiments [M]. New York: John Wiley & Sons, Inc, 2001: 60−119.

[47] DOROZHKIN S V. Calcium orthophosphates ($CaPO_4$): Occurrence and properties [J]. Prog Biomater, 2016, 5: 9−70.

[48] REN Z J, YU F T, GAO H M, CHEN Z J, PENG Y J, LIU L Y. Selective separation of fluorite, barite and calcite with valonea extract and sodium fluosilicate as depressants [J]. Minerals, 2017, 7: 24.

[49] FU F L, WANG Q. Removal of heavy metal ions from wastewaters: A review [J]. Journal of Environmental Management, 2011, 92: 407−418.

[50] YU F L, WANG Y H, ZHANG L, ZHU G L. Role of oleic acid ionic−molecular complexes in the flotation of spodumene [J]. Minerals Engineering, 2015, 71: 7−12.

[51] KUMAR T V V, PRABHAKAR S, RAJU G B. Adsorption of oleic acid at sillimanite/water interface [J]. Journal of Colloid and Interface Science, 2002, 247: 275−281.

[52] PUGH R J. The role of the solution chemistry of dodecylamine and oleic acid collectors in the flotation of fluorite [J]. Colloids and Surfaces, 1986, 18: 19−41.

复合硫化物浮选作业循环水中钙和硫酸根离子去除的热力学及实验研究

Elvis BUSTOS-FLORES, Martha Araceli ELIZONDO-ÁLVAREZ, Alejandro URIBE-SALAS

Department of Metallurgical Engineering, CINVESTAV-IPN, Unidad Saltillo, 25900, Ramos Arizpe, Coahuila, Mexico

摘　要：研究一种用氯化钡($BaCl_2·2H_2O$)和磷酸钠(Na_3PO_4)去除饱和溶液中(0.016 mol/L $CaSO_4$)硫酸钙的化学方法。主要目的是通过沉淀出两种固体物质从溶液中去除这些离子：硫酸根(SO_4^{2-})沉淀为重晶石($BaSO_4$)，钙(Ca^{2+})沉淀为羟基磷灰石($Ca_5(PO_4)_3OH$)。此外，探索一种用油酸和十二烷基胺作捕集剂的固体/液体分离方法(即浮选)。结果表明，在 60 °C、pH 11.5 下用 3.9 g/L $BaCl_2·2H_2O$ 和 1.6 g/L Na_3PO_4 对饱和溶液进行化学处理，促进硫酸钡和缺钙羟基磷灰石($Ca_{10-x}(HPO_4)_x(PO_4)_{6-x}(OH)_{2-x}$)的沉淀，钙和硫酸根的残余浓度分别低于 0.10 和 5 mg/L。当反应剂用量相同、在低于上述温度和 pH 值下处理时，残余钙浓度增加到 28 mg/L。用油酸作捕集剂、pH 9.5 时羟基磷灰石的浮选回收率最高，约为 80%；而用十二烷基胺作捕集剂、pH 6.5 时重晶石的浮选回收率约为 90%。

关键词：钙；硫酸盐；十二烷基胺；油酸；重晶石；羟基磷灰石；浮选分离

(Edited by Wei-ping CHEN)